

1 **A Novel Approach to Detect Accelerated Aged and**
2 **Surface-Mediated Degradation in Explosives by**
3 **UPLC-ESI-MS**

4
5
6 C.L. Crawford*

7
8
9
10 Sandia National Laboratories, Energetics Characterization, PO BOX 5800 – MS 1455
11 Albuquerque, NM USA 87185-1455

12
13
14
15
16
17
18
19
20
21
22
23
24
25 Submitted to:
26 Explosives, Propellants, and Pyrotechnics

27
28 December 2016
29
30
31
32
33
34
35
36
37
38
39
40
41
42

43 *Corresponding Author: Phone 1-505-284-9966; Fax: 1-505-844-5924;
44 email: clcrawf@sandia.gov

1 **ABSTRACT**

2 A new approach was created for studying energetic material degradation. This approach
3 involved detecting and tentatively identifying non-volatile chemical species by liquid
4 chromatography-mass spectrometry (LC-MS) with multivariate statistical data analysis that form
5 as the CL-20 energetic material thermally degraded.

6

7 Multivariate data analysis showed clear separation and clustering of samples based on sample
8 group: either pristine or aged material. Further analysis showed counter-clockwise trends in the
9 principal components analysis (PCA), a type of multivariate data analysis, Scores plots. These
10 trends may indicate that there was a discrete shift in the chemical markers as the went from
11 pristine to aged material, and then again when the aged CL-20 mixed with a potentially
12 incompatible material was thermally aged for 4, 6, or 9 months

13

14 This new approach to studying energetic material degradation should provide greater knowledge
15 of potential degradation markers in these materials.

16

17

18 **KEYWORDS**

19 Accelerated aging; thermal decomposition; CL-20; mass spectrometry; multivariate analysis
20

1 **1 INTRODUCTION**

2 Degradation of energetic materials in explosive components can cause significant changes in an
3 explosive component up to and including failure to function. However, the long term behavior of
4 these materials inside a component microenvironment is still not well understood. The goal of
5 this study was to provide a new approach to detect energetic material degradation. To
6 accomplish this goal, a new analytical method was developed to detect and tentatively identify
7 non-volatile chemical species that form as energetic materials (EM) age and degrade. As
8 molecules degrade, they form both volatile (i.e. gaseous) and non-volatile degradation products.
9 The detection and identification of non-volatile degradation products is an under examined area
10 in the study of energetic material degradation.

11

12 Energetic material degradation has previously been detected by thermal analysis,¹⁻⁴ Fourier
13 transform infrared spectroscopy (FTIR),⁵ secondary ion mass spectrometry (SIMS),⁶ energy
14 dispersive spectroscopy-scanning electron microscopy (EDS-SEM),⁶ and gas chromatography-
15 mass spectrometry.⁷⁻⁹ These methods indicated degradation had occurred but could not determine
16 the identity of the degraded chemical species or why degradation had occurred. In addition, the
17 focus of previous work was on understanding the degradation behavior of the homogenous bulk
18 material. However, bulk material behavior may not be representative of the EM's behavior at the
19 critical initiation surface, i.e. at the bridgewire in an exploding bridgewire (EBW) detonator..
20 Currently, gas analysis (e.g. gas chromatography) and visual inspection are predominantly used
21 at Sandia National Laboratories to assess degradation in aged energetic powders and
22 components, respectively.¹⁰

23

1 Gas analyses can provide semi-quantitative assessments of degradation by tracking the evolution
2 of gases (e.g. N₂, N₂O, NO) as EMs degrade inside a component. Nitrogen containing gases are
3 tracked because most energetic materials have 1 or more nitro (i.e. -NO₂) functional groups. The
4 evolved gases are measured as gas volume from the EM to infer if degradation has occurred (as a
5 ‘rule of thumb,’ if approximately five times the amount of gas is present in the gas analysis of
6 the mixture than is found in the neat materials, the two materials are deemed suspect and
7 potentially incompatible).⁶ Yet, a mass balance equation cannot be used to measure the extent of
8 degradation because current methods do not look for and cannot account for the greatest quantity
9 of degradation products, the non-volatile species. Visual inspection, by definition, is qualitative
10 and subject to instrument (i.e. magnification, lenses, lighting, etc.) and personnel bias. Material
11 degradation, if present in small quantities at the critical initiation surface, may not be visually
12 apparent until gross, bulk degradation begins to occur. Thus, visual inspection is an ‘information
13 only’ type of analysis to assess degradation.

14

15 In order to detect and identify small amounts of non-volatile degradation products in energetic
16 materials, a novel analytical method was created using ultra-high performance liquid-
17 chromatography-electrospray ionization-mass spectrometry (UPLC-ESI-MS). MS has previously
18 been shown to detect and identify non-volatile degradation products in energetic materials but
19 this unique combination of UPLC-ESI-MS has never been applied to the study of degraded
20 energetic material.^{11, 12} This technique was selected for several reasons. First, the UPLC can
21 separate non-volatile species in a mixture, ideally separating EM degradation products away
22 from the bulk EM, i.e. CL-20. Second, the electrospray ionization source creates ions from
23 solubilized chemical species by transferring them into the gas phase. Thus, degradation products

1 that were formed in previous degradation studies but were non-volatile can now be ionized and
2 analyzed by mass spectrometry. Third, the quadrupole time-of-flight (qTOF) mass spectrometer
3 has high detection sensitivity (e.g. a typical limit of detection is parts-per-billion/nanograms
4 gram⁻¹ of material) which is needed to distinguish minor degradation products from the bulk CL-
5 20 material.¹³ Fourth, this technique provides an accurate mass determination of molecules
6 present in a sample. This accurate mass capability helps narrow the choices of potential chemical
7 formulas (e.g. C₅H₁₀O₂) of a molecule from the dozens of empirical formula possibilities and
8 significantly increases the likelihood of accurately identifying a molecule. Finally, this technique
9 can be quantitative if a suitable internal standard, such as ¹⁵N-labelled CL-20, were available. As
10 of now, the technique is semi-quantitative. Together, by detecting and possibly identifying non-
11 volatile degradation products in a chosen material set, this technique can provide a more
12 comprehensive picture of surface-mediated EM degradation than has previously been available.

13

14 The goal of this study was to detect and identify non-volatile degradation products in a model
15 system by UPLC-ESI-MS and highlight differences found in the analysis of pristine CL-20, aged
16 CL-20, and aged CL-20 mixed with SB glass. Samples were created in a sample holder with a
17 similar form factor to an EBW detonator and then underwent accelerated aging for various time
18 periods (4, 6, 9, or 12 months) and temperatures (56°C, 70°C, and 85°C) in thermal conditioning
19 ovens. The following sections describe the experimental details, results, and conclusions from
20 this study.

21

1 **2 EXPERIMENTAL**

2 **2.1 Sample preparation**

3 All of the samples used in this study were created in the Rapid Prototype Facility (RPF) housed
4 in Sandia National Laboratories' (NM) Explosive Technologies Group (ETG). Figure 1 shows
5 the barrel-shaped sample holder that was specifically designed for this project. The barrel-shaped
6 sample holders were designed at Sandia National Laboratories (NM) and were built with 304L
7 stainless steel by Enchanted Machine Works LLC (Albuquerque, NM). The 0.003" thick, 0.35"
8 diameter stainless steel closure disks (not shown) were manufactured by Tech-Etch, Inc.
9 (Plymouth, MA). The closure disks were laser welded onto the sample holders under an Argon
10 cover gas in the ETG's Rapid Prototype Facility. The sample holders then underwent leak
11 testing. A Pfeiffer Vacuum (Nashua, NH) Smart Test helium bombardment leak tester was used
12 to determine the hermeticity of the parts. Each part was tested under a 'pass/fail' regime at $1.0 \times$
13 10^{-8} std.cc sec⁻¹ helium leak rate to check for sample holder hermeticity. The sample holders
14 were also marked with serial numbers using a 75 watt Epilog Helix 24 laser etcher (Epilog Laser,
15 Golden, CO). Gas samples were taken from the top of the holder via a punching device creating
16 a hole in the 0.003" thick closure disk while the powders were extracted from the bottom by
17 removal of the other, 0.003" thick closure disk by machining and then manual extraction of the
18 powder for sample analysis.

19 [Insert Figure 1]

20

21 Table 1 shows the serial number range, number of samples, the energetic and material
22 compatibility type, and the approximate amount of energetic material in each sample. This
23 energetic material amount was based on calculations that maximized the amount of energetic

1 material in the sample while taking into account the volume of the barrel-shaped sample holder
2 and the desired 50% theoretical maximum pressing density of the energetic powder.

3

4 [Insert Table 1]

5

6 **2.2 Thermal aging of samples**

7 Once the samples were created, they were placed in one of three Thermotron (Holland, MI)
8 thermal conditioning ovens housed in the Explosives Technology Group (Albuquerque, NM).

9 The samples were all placed into their respective ovens at the same time. Table 2 below details
10 which samples were placed in which oven, at what temperature (either 56°C, 70°C, or 85°C), and
11 for what length of time. Since the number of ovens was limited and there were other, on-going
12 thermal aging studies being performed, the thermal aging conditions were based on existing
13 thermal set points for these ovens. The timing of the sample pulls was based on previous work
14 conducted by Farrow et al.⁶ A first, test set of samples aged at 85°C were pulled at 4 months to
15 determine if any degradation had occurred. Since there was visual indication of degradation, as
16 seen by digital optical microscopy, the aging study proceeded as planned and the rest of the
17 samples were pulled according to the pull points listed below.

18

19 [Insert table 2]

20

21 **2.2 Gas chromatography/thermal conductivity detection (GC/TCD)** 22 *2.2.1 Analytical method details*

23 Gas analysis was performed on each sample using an Agilent 6890 gas chromatograph (Santa
24 Clara, CA) with thermal conductivity detection (GC/TCD). GC method details are located in

1 appendix A. Briefly, the sample holders were placed in a gas tight sampling manifold and a
2 manual, screw-driven punch was forced through the 0.003" thick closure disk on the top of the
3 sample holder. Once the punch created a hole in the sample holder closure disk, a carrier gas of
4 helium swept the sample gases to the GC inlet for injection into the GC. Liquid nitrogen was
5 used to trap the sample gases as they were being emitted from the holder. After 30 minutes of
6 cold trapping, the gases were then injected onto the GC column via a splitless injection using a
7 15.3 mL min^{-1} helium gas flow. The temperature profile of the GC oven program began by
8 holding -60°C for 5 minutes. The oven temperature then increased at a rate of $12^\circ\text{C min}^{-1}$ to a
9 final temperature of 220°C , with a total run time of 23.33 minutes. A Supelco (Bellefonte, PA)
10 I5302 20' x 1/8" 80/100 Chromasorb 102 column was used for the GC separation. A TCD was
11 used for detection. The detector was set to 250°C with a makeup helium flow rate of 3 mL min^{-1} .
12 30 minute background spectra were collected periodically throughout an analysis period. A
13 background subtraction was performed on all sample gas concentrations to account for trace
14 levels of air present in the background.

15

16 ***2.2.2 GC/TCD data analysis***

17 Automatic peak integration was performed on the chromatographic peaks via the Agilent
18 GC/TCD system software. Peak integration was also manually checked by the author to ensure
19 proper integration of the peaks. The amount of gas produced (μL), an indication of energetic
20 material degradation, was then calculated for each gas species seen in the gas chromatograms.

21

22

1 **2.3 Ultra high pressure liquid chromatography- electrospray**
2 **ionization- mass spectrometry**

3

4 **2.3.1 Explosive standard preparation**

5 100 ppm standards were created by dissolving CL-20 (ATK Launch Systems, Promontory, UT) ,
6 in Fisher Scientific (Waltham, MA) Optima® LC-MS grade acetonitrile (ACN) solvent,
7 respectively. Certified reference materials were not used as analytical standards since these
8 materials were not available. The standards were made up from the original, pristine material that
9 went into the binary samples listed in Table 1 above. The standards were diluted 25x their
10 original concentration using a KD Scientific (Holliston, MA) 2.5 mL borosilicate glass, gas-tight
11 syringe. The syringe was rinsed four times with reagent grade Fisher Scientific ACN solvent and
12 two times with Fisher Scientific Optima® LC-MS grade ACN solvent between explosive
13 standard types to prevent carryover. The standards were made up in Waters (Milford, MA) LC-
14 MS certified 2 mL amber glass vials. All solvents were obtained through Government Scientific
15 Source (Reston, VA) and were used without further purification.

16

17 **2.3.2 Non-explosive standard preparation**

18 A 100 ppm SB glass standard was created by suspending ground, thermally glassed SB glass
19 (Schott North America Inc., Duryea, PA,) in Fisher Scientific Optima® LC-MS grade acetonitrile
20 (ACN) solvent. The standard was diluted 25x its original concentration using a KD Scientific 2.5
21 mL borosilicate glass, gas-tight syringe. The syringe was rinsed four times with Fisher Scientific
22 reagent grade ACN solvent and two times with Fisher Scientific Optima® LC-MS grade ACN
23 solvent between explosive sample types to prevent carryover. The standards were made up in
24 Waters LC-MS certified 2 mL amber glass vials. All samples, except the SB-14 glass powder,

1 were obtained through Government Scientific Source (Reston, VA) and were used without
2 further purification.

3

4 ***2.3.3 Sample preparation***

5 Samples were created by weighing out approximately three milligrams of aged sample material
6 using a NIST traceable Mettler Toledo (Columbus, OH) analytical microbalance. The aged
7 sample material was directly placed into Waters LC-MS 2 mL amber glass vials for analysis. The
8 aged sample material was kept refrigerated in a 4.4°C (40°F) refrigerator until the sample
9 analysis day. On the sample analysis day, the aged sample material was diluted to approximately
10 100 ppm by a 25x dilution using Fisher Scientific Optima® LC-MS grade acetonitrile (ACN)
11 solvent with a KD Scientific (Holliston, MA) 2.5 mL borosilicate glass, gas-tight syringe. The
12 stock solutions did not contain any undissolved material upon visual inspection. The 100 ppm
13 samples for analysis were placed in Waters LC-MS certified 2 mL amber glass vials. The syringe
14 was rinsed four times with reagent grade Fisher Scientific ACN solvent and two times with
15 Fisher Scientific Optima® LC-MS grade ACN solvent between samples to prevent carryover.
16 The samples were run on the day they were created or, if they could not be run on that day, they
17 were stored overnight at 4.4°C to prevent decomposition.

18

19 ***2.3.3 Liquid chromatography experimental conditions***

20 A Waters (Milford, MA) Acquity ultra high pressure liquid chromatograph (UPLC) was used to
21 separate sample species before mass spectral analysis. The UPLC solvent system consisted of 1:1
22 (v:v) Fisher Scientific Optima® LC-MS grade ACN:H₂O. The LC solvent flow rate was 0.4 mL
23 min⁻¹ with an LC injection volume of 2 µL. The LC column temperature was 40°C. The LC

1 column was a Waters Acquity UPLC BEH C18 column with a 1.7 μm particle size. The sample
2 manager was kept at 10°C to reduce sample decomposition. Analytical blanks containing just
3 ACN solvent were run before and after each sample run to prevent sample carryover. The
4 complete UPLC inlet method parameters can be found in appendix A.

5

6 ***2.3.5 Mass spectrometer experimental condition and bass resolution calibration***

7 A Waters Xevo G2 quadrupole time-of-flight mass spectrometer (QTOF-MS) was used for high
8 mass accuracy data collection. This instrument was calibrated for mass resolution in both the
9 positive and negative ion modes before the sample analysis. The reported mass accuracy of the
10 Waters Xevo G2 QTOF-MS was 0.4 ppm for the negative ion mode and 0.2 ppm for the positive
11 ion mode at a 95% confidence interval. A full list of experimental parameters can be found in
12 appendix A.

13

14 ***2.3.5 Negative ion mode UPLC-MS analysis***

15 Negative mode electrospray ionization (ES-) was used to introduce and ionize the samples into
16 the mass spectrometer. Three consecutive (-)UPLC-MS spectra were collected for each sample
17 to demonstrate analytical reproducibility on the analysis day. MS spectra were collected in a 50-
18 1000 Dalton (Da) mass range. Data was collected in the negative ionization mode because CL-20
19 is an electronegative molecule that most easily ionizes in the negative polarity ionization mode.

20

21 ***2.3.6 LC-MS data analysis***

22 LC-MS data was analyzed by Waters (Milford, MA) MarkerLynx XS software. The MarkerLynx
23 software processes LC-MS data sets and builds a results matrix from the data. The results matrix

1 is constructed from the data using an analysis method. Many of the parameters used were default
2 values except for the marker intensity threshold and noise elimination level which were set after
3 several rounds of trial data processing to determine the optimal values for these parameters. The
4 analysis method also contained a mass exclusion list and a mass inclusion list. The mass
5 exclusion list is a list of known m/z values that MarkerLynx XS ignores when searching for
6 markers. These masses are contaminants or prominent mobile phase background peaks. The
7 mass inclusion list is a list of m/z values that are included in the search for unique markers.
8 These lists of m/z values were used to guide the analysis method to either reject or retain certain
9 m/z values, based on the author's knowledge of the ions in the data set. These lists as well as a
10 more detailed description of how MarkerLynx analyzes data are given in appendix A.

11

12 MarkerLynx XS used principal components analysis (PCA) to classify the markers. PCA is a
13 mathematical method that emphasizes the variation in a dataset, allowing patterns within the data
14 to be discerned. PCA finds those components (i.e. markers) that are principal, i.e. that have the
15 largest variance in a data set which produces loadings values. The scores tell how much of each
16 of the components/markers are in a particular sample. Scores data summarize the observations
17 seen in the data, help distinguish signals from noise in the data, and help determine trends,
18 patterns, or groupings in the data.¹⁴ Loadings data summarize the variables. In this data set, the
19 observations were grouped based on the sample type (i.e. pristine CL-20, aged CL-20, and aged
20 CL-20 and SB glass samples) and the variables were made up of the markers identified in each
21 data set (i.e. where a marker represents a unique combination of retention time (minutes), m/z
22 value (Da), and mass spectral peak intensity).

23

1 Plots of scores and loadings data help visualize the grouping in the data and to identify outliers.
2 Scaling is used to account for markers in the data that may dominate and cause discounting of
3 smaller markers. Pareto scaling was used because it reduces the importance of large markers
4 without increasing baseline noise values.¹⁵ The ellipsis gives an indication of the overall
5 grouping of the data in the samples. Samples that fall outside this ellipsis are possible outliers in
6 the data set. The Scores-plot shows samples that have similarities as grouped together. Dissimilar
7 samples are far apart from each other on the plot.

8

9 When performing PCA analyses, cross-validation of the PCA model was critical in ensuring the
10 model does not under-fit or over-fit the data. A cross-validation analysis was performed using
11 the 'leave one out' method of cross-validation.¹⁶ Essentially, one replicate from each sample set
12 was removed from the data set and the PCA analysis was re-run to determine if the remaining
13 data were still grouped together as seen in the previous Scores-plot and the groupings were in the
14 same or similar locations on the new Scores-plot. As expected, the sample groups were
15 predominantly found in the same location. This similar grouping of the data indicates that the
16 original PCA model is neither over-fitting nor under-fitting the sample data.

17

18 Orthogonal partial least squares-discriminant analysis (OPLS-DA) was also used to perform
19 pairwise analyses (e.g. pristine CL-20 and aged CL-20). OPLS-DA loadings data can be
20 visualized using an s-plot. An s-plot is used to visualize the OPLS-DA loadings data by
21 combining the OPLS-DA modelled covariance and correlation in a scatter plot.¹⁴ The p₁-axis
22 describes the variable magnitude. The p_(corr)₁-axis describes the reliability of each variable in
23 X. Markers at either (-1,-1) or (1,1) have high magnitude and high reliability; these markers are

1 the most statistically significant, i.e. these markers are the most distinct or dissimilar from the
2 markers in the other sample group. The accuracy of an s-plot is influenced by the number of
3 markers in a sample set. Sample sets with many markers tend to reduce the scatter in the plot and
4 create the typical ‘S’ shaped data distribution on the plot; very noisy sample sets tend to increase
5 the scatter in the data, even if a large amount of samples are present. The noise in this sample set
6 was 12%.

7

1 3 RESULTS

2 3.1 GC/TCD analysis results

3 After accelerated aging, the samples underwent gas analysis via gas chromatography/thermal
4 conductivity detection. Overall, as shown in Figure 2, the gas analysis results showed that more
5 gas was generated in samples aged at 85°C with lower amounts in the 70°C and 56°C samples,
6 respectively. This result was expected and agreed with earlier gas analysis studies with this
7 material set.⁶ The gas analysis results also indicated a separate degradation mechanism may be
8 occurring at 85°C than at 56°C or 70°C.

9
10 Several trends emerge from the summary data. Generally, the 85°C samples had approximately
11 four times as many moles of N-containing degradation products than the 70°C samples. The
12 70°C samples had approximately two to three times as many moles of N-containing degradation
13 products than the 56°C samples. Figure 2 shows that, among the samples aged at 85°C (squares),
14 the samples aged for 6 and 9 months had larger amounts of nitrogen-containing gas species
15 (series of squares) attributed to degradation than the samples aged for 4 months. This same trend
16 also held true for the 56°C (circles) and 70°C samples (triangles), respectively. These trends
17 were expected and have been seen previously.⁶ The presence of these trends confirmed that the
18 thermal aging regime successfully induced accelerated aging of the CL-20 when in the presence
19 of SB glass. Taken alone, the gas analysis results provide a semi-quantitative indicator that
20 degradation has occurred in the CL-20 but identifying both the volatile and non-volatile
21 degradation products is not possible with this technique.

22
23 [insert figure 2]
24

1 **3.2 LC-MS results**

2 Once the samples had undergone gas analysis and visual inspection, they were analyzed by
3 UPLC-ESI-MS. The initial review of the LC data showed that different chemical species were
4 present depending on the sample material type (pristine or aged) and sample composition (CL-20
5 or CL-20 mixed with SB glass).

6

7 After determining chromatographic reproducibility and that the chromatograms appeared to have
8 the same peaks at the same retention times across the various aging temperatures, the raw mass
9 spectra were analyzed for each chromatographic peak in a CL-20 and SB glass sample aged for 9
10 months at 85°C (shown in figure 11C above). Figure 3 shows a representative total ion
11 chromatogram (TIC) (figure 3A) along with this chromatogram's corresponding mass spectra for
12 the chromatographic peaks at 0.47 (figure 3B, ▲), 1.09 (figure 3C, ●), 1.52 (figure 3D, ■), and
13 2.14 (figure 3E, ★) minutes, respectively. The accompanying mass spectra show the ionic species
14 present in the sample. These mass spectra illustrate the variety of ionic species produced in this
15 sample across the chromatographic run. Several species represented mobile phase contaminants
16 that were present in every liquid chromatographic run, i.e. 94.97 Da. but these masses were
17 subtracted from the sample spectra before any multivariate statistical analysis of the data. The
18 peak at 2.14 minutes has several co-eluting species, one or more of which may be a degraded
19 form of CL-20 while undegraded CL-20 is also present. Other spectra (not shown) showed that
20 not only are the MS spectra for the peak at 2.14 minutes reproducible across the various
21 temperatures but are also reproducible for the other three chromatographic peaks in the LC
22 spectrum (i.e. 0.47 minutes, 1.09 minutes, and 1.52 minutes). Since the elution times for the LC
23 peaks are the same and the MS peaks within the LC peaks are the same, this result seems to
24 indicate the chemical degradation mechanism is the same across all three temperatures studied.

1 However, further analysis by PCA will show that this may not be a complete description of the
2 data.

3

4 [Insert figure 3]

5

6 *3.2.1 Principal Components Analysis (PCA) of the LC-MS data*

7 While the analysis of the liquid chromatographic and mass spectral data showed few differences
8 in the type of ion species found across the samples aged at various temperatures and time
9 periods, further data analysis by principal component analysis (PCA) was used to find trends in
10 the data not obvious via the preceding, traditional chromatographic and mass spectral peak
11 interpretation. In particular, PCA can discern differences in the signal intensities of the major ion
12 species, the presence or absence of minor ion species, and outliers in the sample data.

13

14 Figure 4 shows a scores-plot generated by the PCA analysis of the various time and temperature
15 samples for CL-20 and SB glass. The PCA analysis differentiated three distinct sample groups:
16 pristine CL-20 (top, left quadrant); aged CL-20 (lower, left quadrant), and aged CL-20 and SB
17 glass. This analysis revealed the presence of these groupings, which was not readily apparent by
18 traditional, 2D LC-MS data interpretation and indicated that the chemical markers in these
19 sample sets were distinctly different from each other to produce the three separate data clusters.

20

21 [insert figure 4]

22

1 Additionally, as seen in Figure 5A, the samples aged at 85 °C cluster together and were arranged
2 in a semi-circular, counter-clockwise pattern. This circular pattern indicates that there was a
3 discrete shift in the chemical markers as the CL-20 went from pristine to aged material, and then
4 again when the aged CL-20 mixed with SB glass was aged for 4, 6, or 9 months. Figure 5B
5 shows the same semi-circular, counter-clockwise pattern for the 70 °C sample set. Interestingly,
6 figure 5C shows what looks like a semi-circular, *clockwise* pattern for the 56 °C sample set. This
7 reversal in the direction of the pattern may indicate a different chemical degradation mechanism
8 from the mechanism(s) at 70 °C and 85 °C. These circular trends have been seen in other PCA
9 analyses of chemical markers, most notably in the metabolic biomarkers of fasting rats and rats
10 1-6 hours after feeding.¹⁷

11

12 [Insert figure 5]

13

14 **3.2.2 Orthogonal Partial Least Squares- Discriminant Analysis (OPLS-DA) of the LC-MS
15 data and Trend Plots**

16 Orthogonal partial least squares- discriminant analysis (OPLS-DA) was used to find similarities
17 or differences between two sample groups. OPLS-DA is used to find in-group variation and
18 between-group variation., i.e. to find variance or to discriminate between groups and to identify
19 markers that influenced the separation of two sample groups.

20

21 Figure 6A shows an s-plot for the OPLS-DA comparison of pristine Cl-20 and CL-20 aged at
22 85°C for 4 months. The markers highlighted in the red squares were the most statistically
23 significant data in the plot since they are grouped at either (-1,-1) or (1,1). These highlighted

1 species were the ions present in each sample that were the most statistically dissimilar from each
2 other. From this analysis, it was possible to tentatively identify the chemical species which most
3 heavily influenced the separation between sample groups from each other and were identified as
4 potential markers of degradation in table 3. These plots compared CL-20 aged at 85°C for 4
5 months vs. CL-20 mixed with SB glass aged at 85°C for 4 months and CL-20 mixed with SB
6 glass aged for 4 months at 85°C vs. CL-20 mixed with SB glass aged for 9 months at 85°C.
7 Further studies will help to verify and validate that these species are the likeliest candidates
8 contributing to the degradation of the CL-20 by the glass.

9

10 [Insert figure 6]
11

12 When analyzing the most significant markers from the s-plots (the values boxed in the upper
13 right hand corner and lower left hand corner of figure 6A), several trends emerged. Figure 6B
14 shows a trend plot which illustrates the relative mass spectral peak intensity (%) and how this
15 peak intensity influenced clustering of various sample groups in the PCA analysis for a specific
16 marker across all the samples in a sample set. This plot shows the mass spectral peak intensity
17 for the marker at m/z 500.00 and a chromatographic retention time of 2.14 minutes. For this
18 particular marker, the peak intensities are lowest in the pristine and aged CL-20 while the marker
19 intensity is higher in all the samples of aged CL-20 mixed with glass. The m/z 500.00 ion was
20 due to $[CL-20+NO_3]^-$. One theory that may explain this trend is that the SB glass is catalyzing
21 the natural degradation of CL-20 to produce nitrate, which is then readily available as an adduct
22 species for the remaining CL-20 still left in the sample. In the pristine, QC, and aged CL-20
23 samples, the natural degradation of CL-20 is proceeding at a slower rate. Thus, there is less
24 nitrate to adduct with the CL-20 and produce this characteristic m/z 500 ion. There may also be

1 higher amounts of residual nitrate in the SB glass that could have contributed to the trend in mass
2 spectral peak intensity seen in the plot.

3
4 Table 3 lists the major ion species identified via the s-plot shown in figure 6A. Where possible,
5 the mass spectral peaks were identified based on their exact mass and the peak patterns generated
6 in the mass spectra seen previously. The ^{35}Cl and ^{37}Cl adduct ion species were identified using
7 predicted isotope ratio spectra which, in addition to the exact mass calculation, helped to
8 correctly identify these peaks. The chloride ion source is most likely from the SB glass and the
9 LC solvents.

10
11 The table shows that the chromatographic peak at 0.47 minutes yielded a major ion species at
12 m/z 200.0054. This species could not be identified but may be related to a CL-20 degradation
13 product forming an adduct ion with another species in the sample. The chromatographic peak at
14 1.09 minutes, which was only seen in the chromatograms for the samples of aged CL-20 with SB
15 glass, yielded three major ions. Only one of these ions, m/z 94.97, could be identified as a
16 common contaminant in liquid chromatography. The other ions present in this peak may be
17 related to a CL-20 degradation product but this mass spectral peak analysis could not definitively
18 identify them.

19 The ion species that made up the chromatographic peak at 1.52 minutes were assigned to ion
20 species from an under-nitrated, synthetic by-product of the synthesis of CL-20, 2-acetyl-
21 4,6,8,10,12-pentanitro-2,4,6,8,10,12-hexaazaisowurtzitane or the ‘mono-acetyl’ species.¹⁸ This
22 species was present in all CL-20 samples tested, i.e. the pristine CL-20, the aged CL-20, and the
23 aged CL-20 and glass samples. This result indicates that the mono-acetyl product may serve as

1 an inadvertent internal standard in CL-20 powder and may be useful in future studies. Another
2 interesting finding is that the mono-acetyl species formed gas-phase dimers. The formation of
3 gas-phase dimers of these species has not previously been reported. This result indicates that the
4 mono-acetyl concentration was abundant enough to form dimers or that the mono-acetyl species
5 is prone to dimer formation, which is relatively rare for negative mode ionization. UPLC/PDA
6 analysis of CL-20 for purity has indicated that less than 1% of any under-nitrated, synthetic
7 byproducts were present in the SNL EBW grade CL-20.¹⁹ The result from this study indicated
8 that this material is present in the CL-20 but may be below the detection limits for the typical
9 UPLC/PDA method of analysis.¹⁸

10

11 The ion species that made up the chromatographic peak at 2.14 minutes consisted of ions related
12 to CL-20 and possibly minor amounts of CL-20 degradation products. The adduct species (e.g.
13 CL-20+Cl⁻, CL-20+NO₃⁻, etc.) were similar to the adducts formed with the mono-acetyl species.
14 In particular, the species at 2.14 minutes, m/z 436.02 may be the hydrolysis product of CL-20
15 degradation predicted by Qasim *et al.* in his *ab initio* calculations of CL-20 degradation.^{6,20}

16

17 The CL-20 species also formed gas-phase dimers which also has not previously been reported.
18 The mass spectra also indicated the presence of unidentified species and minor species not listed
19 in the table. However, these species can have an effect on multivariate analysis of the aged
20 sample material.

21

22

1 **4 Conclusions**

2 The use of UPLC-ESI-MS along with multivariate statistical analysis showed that even small
3 amounts of thermal degradation can be detected using this approach. This novel approach to
4 analyzing organic materials for degradation also showed that the amount of time and temperature
5 of the accelerated aging regime influenced the extent of degradation and possibly the type of
6 degradation products formed. Now that several markers of degradation have been identified for
7 the CL-20/SB glass material set, further work should be conducted to more accurately probe how
8 these and perhaps other markers form as part of SB glass-induced degradation and CL-20
9 thermal degradation. This work may eventually provide mechanistic information to determine
10 how and why SB glass induces and/or accelerates degradation of CL-20 and may be used to
11 benchmark *ab initio* molecular dynamics simulations of CL-20 degradation. This technique may
12 also be useful as an early-warning diagnostic to find evidence of EM degradation before changes
13 in bulk material are evident.

14

15 Another innovation resulting from this project included the use of a new, hermetically sealed
16 sample holder that improved upon current gas sample collection apparatus (i.e. POTs). These
17 sample holders proved useful for tandem GC/TCD and UPLC-ESI-MS analysis and they should
18 be used in future aging and compatibility studies where both gas and non-volatile degradation
19 products collection is desired.

20

21 In summary, this study is the first to apply recently available and more sensitive UPLC-ESI-MS
22 with multivariate statistical data analysis to better understand how surface-mediated EM
23 degradation occurs in the CL-20/SB glass material set. This technique and data analysis method

1 probed the previously under examined non-volatile degradation products in CL-20, a key
2 deficiency in our knowledge of this energetic material's degradation properties. This knowledge
3 of potential degradation markers may enable new and more accurate experimental and
4 computational methods to predict degradation in CL-20 and possibly other energetic materials.

5

6 **5 Acknowledgements**

7 This project was supported by the Laboratory Directed Research and Development program at
8 Sandia National Laboratories, a multi-program laboratory managed and operated by Sandia
9 Corporation, a wholly owned subsidiary of Lockheed Martin Corporation, for the U.S.
10 Department of Energy's National Nuclear Security Administration under contract DE-AC04-
11 94AL85000. The author would also like to thank her co-workers in the Explosive Technologies
12 Group at Sandia National Laboratories for their support of this work.

13

1 6 REFERENCES

- 2 1. J.W. Bulluck and R.A. Rushing, *Interim Report On Chemical And Thermal Analysis of*
3 *Coflon*, International Research Project on the Effects of Chemical Ageing of Polymers on
4 Performance Properties, TRI: Austin, TX 1994.
- 5 2. F. Volk, *Determination of Gaseous and Solid Decomposition Products of Nitroguanidine*.
6 Propellants, Explosives, Pyrotechnics, 1985. 10(5): p. 139-146.
- 7 3. G. Anderson and M. Scott, *Determination of Product Shelf Life and Activation Energy*
8 *for Five Drugs of Abuse*. Clinical Chemistry, 1991. 37(3): p. 395-402.
- 9 4. R. Turcotte, M. Vachon, Q.S.M. Kwok, R. Wang, and D.E.G. Jones, *Thermal study of*
10 *HNIW (CL-20)*. Thermochimica Acta, 2005. 433: p. 105-115.
- 11 5. D.M. Haaland and G.E. Rivord, *High Resolution Fourier Transform Infrared*
12 *Spectroscopy For The Investigation of Decomposition Gases Generated by Aging*
13 *Organic Materials*, SAND79-0935C, Sandia National Laboratories: Albuquerque, NM
14 1979.
- 15 6. M. Farrow, *Materials Evaluation of the Use of CL-20 in Exploding Bridge Wire*
16 *Detonators*, SAND2015-4090, Albuquerque, NM: Albuquerque, NM 2015.
- 17 7. M.R.L. Paine, P.J. Barker, S.A. MacLuglin, T.W. Mitchell, and S.J. Blanksby, *Direct*
18 *detection of additives and degradation products from polymers by liquid extraction*
19 *surface analysis employing chip-based nanospray mass spectrometry*. Rapid Commun.
20 Mass Spectrom., 2011. 26: p. 412-418.
- 21 8. G.V.W. II, J.N. Smith, R.L. Clough, J.A. Ohlhausen, J.M. Hochrein, and R. Bernstein,
22 *The origins of CO₂ and NH₃ in the thermal-oxidative degradation of nylon 6.6*. Polymer
23 Degradation and Stability, 2012. 97: p. 1396-1404.
- 24 9. J.N. Smith, G.V.W. II, M.I. White, R. Bernstein, and J.M. Hochrein, *Characterization of*
25 *Volatile Nylon 6.6 Thermal-Oxidative Degradation Products by Selective Isotopic*
26 *Labeling and Cryo-GC/MS*. Journal of the American Society for Mass Spectrometry,
27 2012. 23: p. 1579-1592.
- 28 10. M. Farrow, *[OUO] Accelerated Aging of the MC4754*, CL-20 Technical Review
29 Meeting, Sandia National Laboratories 2010.
- 30 11. G.W. Brown and A.M. Giambra, *HPLC-MS Examination of Impurities in Pentaerythritol*
31 *Tetranitrate*. Journal of Energetic Materials, 2014. 32: p. 117-128.
- 32 12. M.R.L. Paine, B.B. Kirk, S. Ellis-Steinborner, and S.J. Blanksby, *Fragmentation*
33 *pathways of 2,3-dimethyl-2,3-dinitrobutane cations in the gas phase*. Rapid
34 Communications in Mass Spectrometry, 2009. 23(18): p. 2867-2877.
- 35 13. G.L. Glish and R.W. Vachet, *The basics of mass spectrometry in the twenty-first century*.
36 Nat Rev Drug Discov, 2003. 2(2): p. 140-150.
- 37 14. S. Wiklund (2008) *Multivariate Data Analysis for Omics*.
- 38 15. B. Worley and R. Powers, *Multivariate Analysis in Metabolomics*. Current
39 Metabolomics, 2013. 1(1): p. 92-107.
- 40 16. R. Bro, K. Kjeldahl, A.K. Smilde, and H.A.L. Kiers, *Cross-validation of component*
41 *models: A critical look at current methods*. Analytical and Bioanalytical Chemistry,
42 2008. 390: p. 1241-1251.
- 43 17. K. Kaplan, P. Dwivedi, S. Davidson, Q. Yang, P. Tso, W. Siems, and H.H. Hill,
44 *Monitoring Dynamic Changes in Lymph Metabolome of Fasting and Fed Rats by*
45 *Electrospray Ionization-Ion Mobility Mass Spectrometry (ESI-IMMS)*. Analytical
46 Chemistry, 2009. 81(19): p. 7944-7953.

1 18. NATO, *STANAG 4566 JAS (Edition 1)- Explosives, Specification for ϵ -CL-20*
2 (*Hexanitrohexaazaisowurtzitane*) *for Deliveries from One NATO Nation to Another*, N.S.
3 Agency, Editor: Brussels, Belgium.

4 19. M. Farrow, D.M. Rosenberg, and J.R. Tucker, *Specification, CL-20, Initiating Increment*
5 *Material for Exploding Bridgewire Detonators* Sandia National Laboratories:
6 Albuquerque, NM.

7 20. M. Qasim, H. Fredrickson, C. McGrath, J. Furey, J. Szecsody, and R. Bajpai,
8 *Semiempirical Predictions of Chemical Degradation Reaction Mechanisms of CL-20 as*
9 *Related to Molecular Structure*. *Structural Chemistry*, 2004. 15(5): p. 493-499.

10 21. A. Savitzky and M.J.E. Golay, *Smoothing and Differentiation of Data by Simplified Least*
11 *Squares Procedures*. *Analytical Chemistry*, 1964. 36(8): p. 1627-1639.

12

13

1 **FIGURE CAPTIONS**

2

3 Figure 1. CAD drawing of the barrel-shaped sample holder designed for this project. The sample
4 material was loaded into the lower, wider section of the sample holder so that the punching tool
5 used in the gas analysis would punch the top closure disk and not come into contact with the
6 energetic material.

7

8 Figure 2. Summary of the gas analysis data collected for samples containing CL-20 and SB glass
9 aged at either 56°C, 70°C or 85°C for 4, 6, 9, or 12 months.

10

11 Figure 3. A)Total ion chromatogram (TIC) with relative peak intensity (%) vs. chromatographic
12 run time (minutes) for CL-20 and SB glass aged for 9 months at 85°C. The spectra were
13 smoothed using a Savitsky-Golay 1x1 smoothing algorithm;²¹ B) averaged mass spectrum of the
14 chemical species eluting at 0.47 minutes (▲); C) averaged mass spectrum of the species eluting
15 at 1.09 minutes (●); D) averaged mass spectrum of the species eluting at 1.52 minutes
16 (■);averaged mass spectrum of the species eluting at 2.14 minutes (★).

17

18 Figure 4. Scores-plot with principal component 1 ($t(1)$) on the x-axis and principal component 2
19 ($t(2)$) on the y-axis. This scores-plot represents pristine CL-20 (top, left quadrant), CL-20 aged
20 for 4 months at 85°C (lower, left quadrant), and CL-20 mixed with glass and aged for 4, 6, 9 or
21 12 months at either 56°C, 70°C, or 85°C.

22

23 Figure 5. A)Scores-plot with principal component 1 ($t(1)$) on the x-axis and principal component
24 2 ($t(2)$) on the y-axis. This scores-plot shows the counter-clockwise pattern formed between
25 pristine CL-20 (top, left quadrant), CL-20 aged for 4 months at 85°C (lower, left quadrant), and
26 CL-20 mixed with glass and aged for 4, 6, or 9 months at 85°C. B) This scores-plot shows the
27 counter-clockwise pattern formed between pristine CL-20 (top, left quadrant), CL-20 aged for 4
28 months at 85°C (lower, left quadrant), and CL-20 mixed with glass and aged for 6, 9, or 12
29 months at 70°C. C) This scores-plot shows the counter-clockwise pattern formed between
30 pristine CL-20 (top, left quadrant), CL-20 aged for 4 months at 85 °C (lower, left quadrant), and
31 CL-20 mixed with glass and aged for 6, 9, or 12 months at 56 °C.

32

33 Figure 6. A) An s-plot displaying the $p(\text{corr})_1$ values versus OPLS-regression coefficients for
34 pristine CL-20 vs CL-20 aged at 85°C for 4 months. B) Plot of mass spectral peak intensity (%)
35 vs. sample group for the marker at m/z 500.00 and a chromatographic retention time of 2.14
36 minutes. Errors bars are given at $\pm 1\sigma$.

1 **TABLES**

2 Table 1. Sample information

S/N	# of samples	Energetic material	Material compatibility sample	Approx. EM material amt. (mg) <i>per sample holder</i>
01-15	15	CL-20	SB glass	95 mg
71	1 (control)	CL-20	--	190 mg
74	1 (control)	--	SB glass	190 mg
79	1 (control)	CL-20	--	185 mg

3

4 Table 2. Thermal Conditioning Sample Pull Chart

	<i>85°C oven</i> <i>Model #: S-16C, SN 25048</i>	<i>70°C oven</i> <i>Model #: S-5.5H, SN 21908</i>	<i>56°C oven</i> <i>Model # S-16C, SN 25046</i>
4 mo.	6, 12, 71, 74, and 79	-----	-----
6 mo.	8	5, 9	3, 10
9 mo.	15	11	1
12 mo.	-----	14	13

5

6

1 Table 3. Peak table for the major ion species found in the analysis of aged of CL-20 and SB glass
 2 aged for 9 months at 56°C

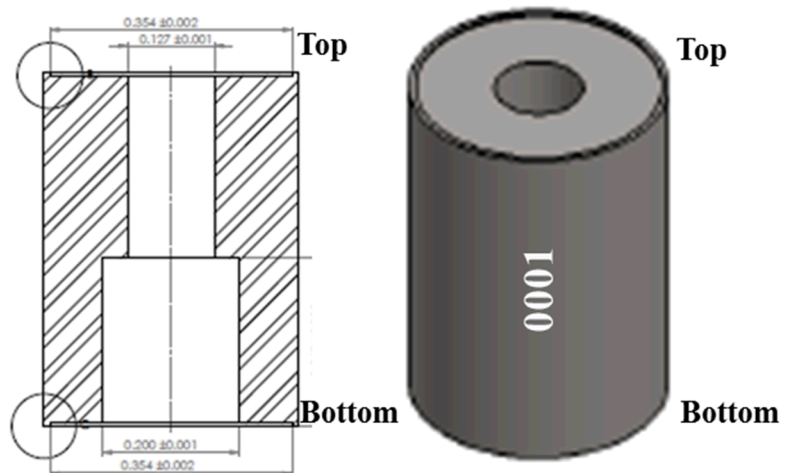
Retention Time (min.)	Measured m/z (Da.)	Exact mass (Da.)	Tentative peak ID	Elemental composition
0.47	200.0054	--	?	--
1.09	94.9792	95.9881	Methanesulfonate	CH ₃ SO ₃ H
	115.0765	--	?	--
	311.1661	--	?	--
1.52	434.0445	434.0405	(X-H) ⁻	C ₈ H ₈ N ₁₁ O ₁₁
	--	435.0483	X*	C ₈ H ₉ N ₁₁ O ₁₁
	470.0164	470.0172	(X+ ³⁵ Cl) ⁻	C ₈ H ₉ N ₁₁ O ₁₁ ³⁵ Cl
	472.0143	472.0142	(X+ ³⁷ Cl) ⁻	C ₈ H ₉ N ₁₁ O ₁₁ ³⁷ Cl
	497.0364	497.0361	(X+NO ₃) ⁻	C ₈ H ₉ N ₁₂ O ₁₄
	551.9728	N/A	?	--
	905.0733	905.0655	(X ₂ + ³⁵ Cl) ⁻	C ₁₆ H ₁₈ N ₂₂ O ₂₂ ³⁵ Cl
	907.0667	907.0625	(X ₂ + ³⁷ Cl) ⁻	C ₁₆ H ₁₈ N ₂₂ O ₂₂ ³⁷ Cl
	932.0778	932.0844	(X ₂ +NO ₃) ⁻	C ₁₆ H ₁₈ N ₂₃ O ₂₅
2.14	436.0201	436.0197	(M-NO ₂ -H ₂ O+NO ₃) ⁻	C ₇ H ₆ N ₁₁ O ₁₂
	437.0139		(M-H) ⁻	C ₆ H ₅ N ₁₂ O ₁₂
	--	438.0228	M=CL20	C ₆ H ₆ N ₁₂ O ₁₂
	453.0071	--	?	--
	472.9902	472.9916	(M+ ³⁵ Cl) ⁻	C ₆ H ₆ N ₁₂ O ₁₂ ³⁵ Cl
	474.9899	474.9887	(M+ ³⁷ Cl) ⁻	C ₆ H ₆ N ₁₂ O ₁₂ ³⁷ Cl
	500.0119	500.0106	(M+NO ₃) ⁻	C ₆ H ₆ N ₁₃ O ₁₅
	911.0167	911.0145	(M ₂ + ³⁵ Cl) ⁻	C ₁₂ H ₁₂ N ₂₄ O ₂₄ ³⁵ Cl
	913.0165	913.0115	(M ₂ + ³⁷ Cl) ⁻	C ₁₂ H ₁₂ N ₂₄ O ₂₄ ³⁷ Cl
	921.0442	921.0307	((M-H)M+NO ₂) ⁻	C ₁₂ H ₁₁ N ₂₅ O ₂₆
	937.0355	937.0256	((M-H)M+NO ₃) ⁻	C ₁₂ H ₁₁ N ₂₅ O ₂₇
	938.0336	938.0334	(M ₂ +NO ₃) ⁻	C ₁₂ H ₁₂ N ₂₅ O ₂₇

3 *X is 2-acetyl-4,6,8,10,12-pantanitro-2,4,6,8,10,12-hexaazaisowurtzitane, an under-nitrated, synthetic by-product of
 4 the synthesis of CL-20.

5
 6

1 **FIGURES**

2 Figure 1

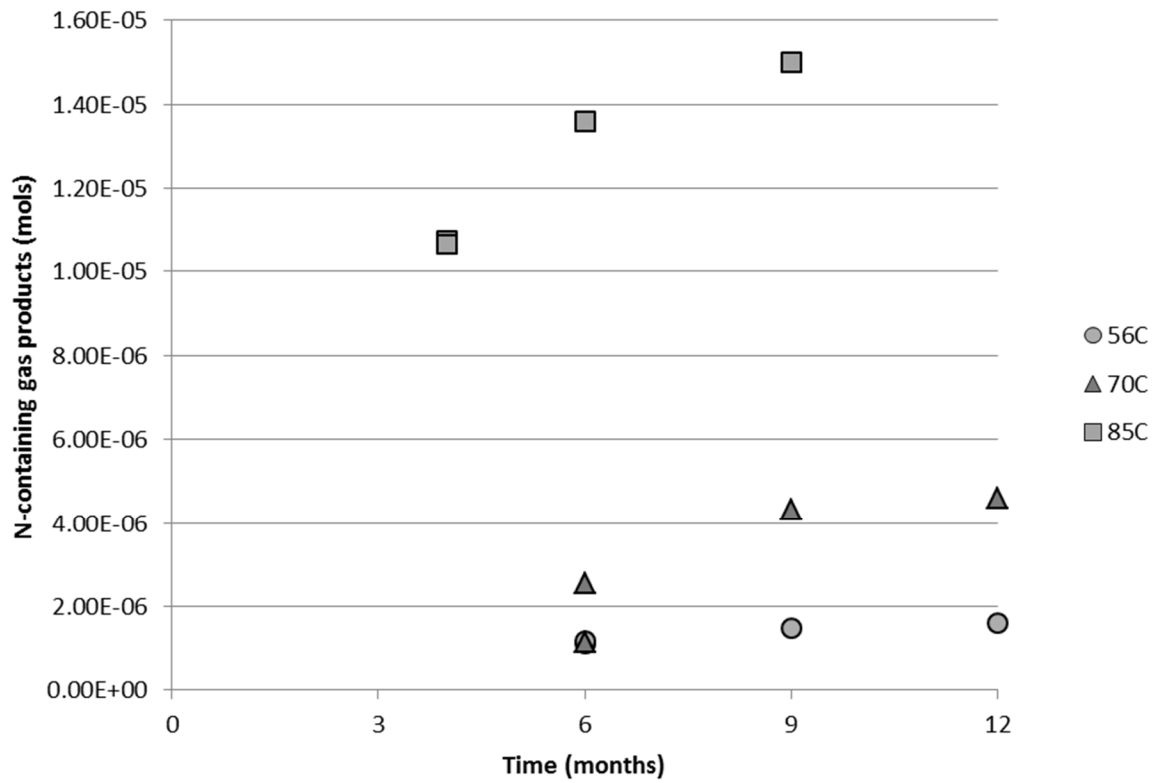


3

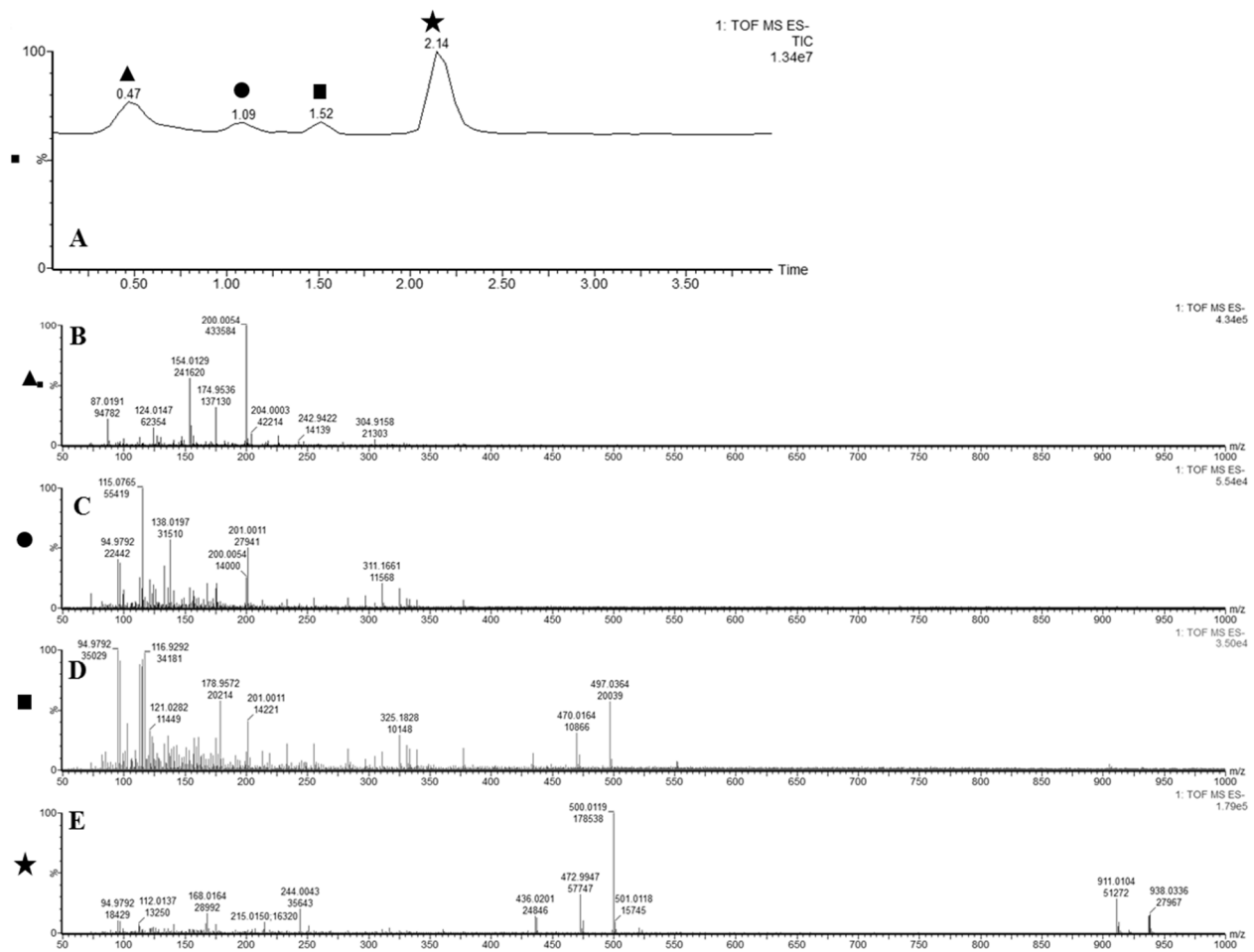
4

5

1 Figure 2
2



1 Figure 3

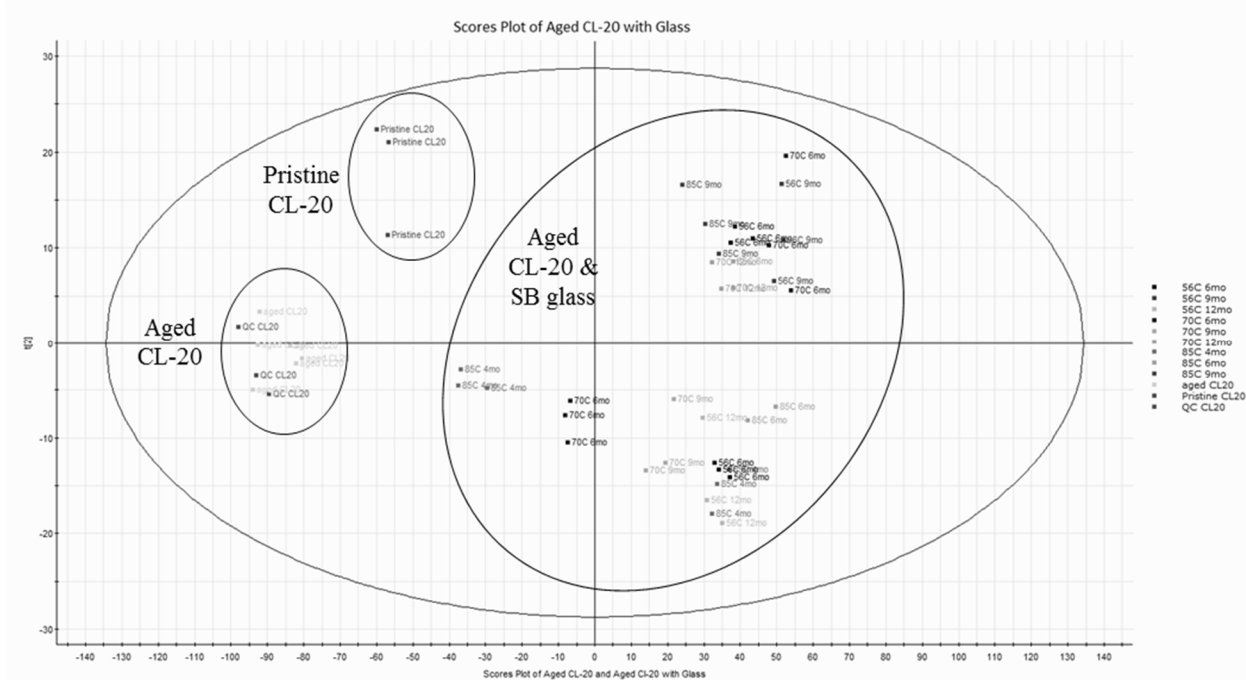


2

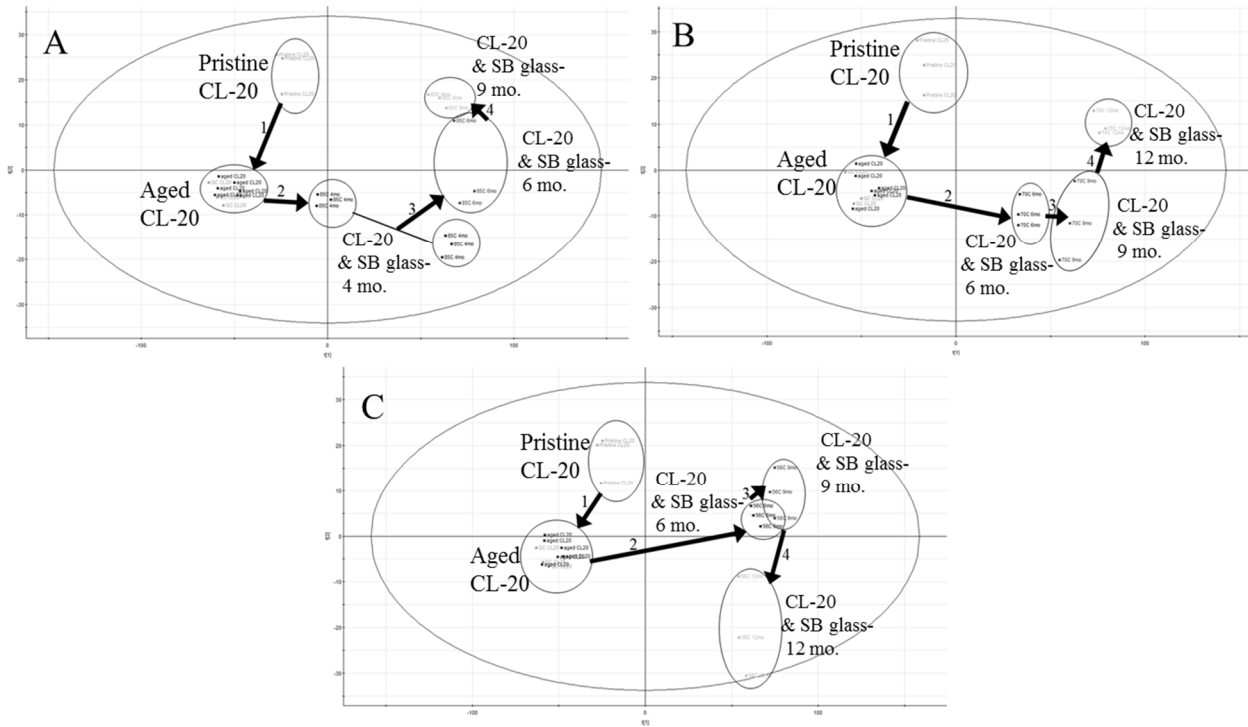
3

4

1 Figure 4



1 Figure 5



2

3

1 Figure 6

